Supplement for

"Validity and limitations of simple reaction kinetics to calculate concentrations of organic compounds from ion counts in PTR-MS"

by

Rupert Holzinger[1], W. Joe F. Acton[2], William J. Bloss[3], Martin Breitenlechner[4], Leigh R. Crilley[3], Sébastien Dusanter[5], Marc Gonin[6], Valerie Gros[7], Frank N. Keutsch[4], Astrid Kiendler-Scharr[8], Louisa J. Kramer[3], Jordan E. Krechmer[9], Baptiste Languille[7], Nadine Locoge[5],Felipe Lopez-Hilfiker[6], Dušan Materić[1], Sergi Moreno[10], Eiko Nemitz[11], Lauriane L.J. Quéléver[12], Roland Sarda Esteve[7], Stéphane Sauvage[5], Simon Schallhart[13,a], Roberto Sommariva[3], Ralf Tillmann[8], Sergej Wedel[8], David R. Worton[10], Kangming Xu[1], Alexander Zaytsev[4]

[1] Institute for Marine and Atmospheric Research, Utrecht, IMAU, Utrecht University, the Netherlands.
[2] Lancaster Environment Centre, Lancaster University, Lancaster, LA1 4YQ, UK.
[3] School of Geography, Earth and Environmental Sciences, University of Birmingham, Birmingham, B15 2TT, UK.
[4] John A. Paulson School of Engineering and Applied Sciences, Harvard University, Cambridge, MA 02138, USA
[5] IMT Lille Douai, Université Lille, SAGE - Département Sciences de l'Atmosphère et Génie de l'Environnement, F-59000
[6] TOFWERK AG, Switzerland
[7] LSCE, Laboratoire des Sciences du Climat et de l'Environnement, Unité Mixte CEA-CNRS-UVSQ, IPSL, CEA/Orme des Merisiers, 91191 Gif-sur-Yvette, France.
[8]Institute of Energy and Climate Research, IEK-8: Troposphere, Forschungszentrum Jülich GmbH, Jülich, Germany
[9] Aerodyne Research Inc. Billerica, MA, 01821 USA
[10] National Physical Laboratory, Hampton Road, Teddington, Middlesex, TW11 0LW, UK.
Lille, France.
[11] Centre for Ecology & Hydrology, CEH, Bush Estate, Penicuik, Midlothian, EH26 0QB, UK.
[12] Institute for Atmospheric and Earth System Research - INAR/ Physics, P.O. Box 64, FI-00014 University of Helsinki, Finland.
[13] Finnish Meteorological Institute, P.O. Box 503, FI-00101 Helsinki, Finland.

[a] now at: Finnish Meteorological Institute, Helsinki, Finland

Correspondence to: Rupert Holzinger (r.holzinger@uu.nl)

Table S1. Specifications of the NPL gas standard that was used September 23 through 28, 2017.

Compound	**VMR ± uncertainty [nmol/mol]**	**Formula**	***m/Q* protonated[1] [Th]**	***m/Q* fragments [Th]**
methanol	1019±31	CH_4O	33.033	-
acetonitrile	1020±31	CH_3CN	42.034	-
acetaldehyde	1001±30	C_2H_4O	45.033	-
acetone	983±20	C_3H_6O	59.049	
isoprene	996±20	C_5H_8	69.070	41.039
methylvinylketone	961±29	C_4H_6O	71.049	
methylethylketone	1009±30	C_4H_8O	73.065	
benzene	1025±15	C_6H_6	79.054	
m-xylene	998±25	C_8H_{10}	107.086	
1,2,4-trimethylbenzene	1001±25	C_9H_{12}	121.101	
3-carene	989±25	$C_{10}H_{16}$	137.132, 138.136	81.070
1,2,4-trifluorobenzene	1047±52	$C_6H_3F_3$	133.026	
octamethylcyclo-tetrasiloxane (D4)	901±45	$C_8H_{24}Si_4O_4$	297.083, 298.082, 299.079	281.051, 282.051, 283.048
decamethylcyclo-pentasiloxane (D5)	1051±53	$C_{10}H_{30}Si_5O_5$	371.101, 372.101, 372.105, 373.098	355.070, 356.070, 357.067
propane	981±15	C_3H_8	Not detected	

[1] *m/Q* values of isotopologues are only listed if their relative abundance is at least 10% of the most abundant isotopologue.

Table S2. Specifications of the Apel-Riemer gas standard used September 18 through 22, 2017. This standard has been re-filled into a stainless-steel cylinder (2 L, 2000 psi), which is likely the reason that a large fraction of acetaldehyde has been lost. Therefore, we used an acetaldehyde mixing ratio of 600 nmol/mol for all calculations. All other mixing ratios were found to be consistent between the two gas standards.

Compound	**VMR (uncertainty is ±5%) [nmol/mol]**	**Formula**	***m/Q* protonated[1] [Th]**	***m/Q* fragments [Th]**
methanol	1011	CH_4O	33.033	-
acetonitrile	1010	CH_3CN	42.034	-
acetaldehyde	1111	C_2H_4O	45.033	-
acetone	967	C_3H_6O	59.049	
2-methyl-buten-2-ol	998	$C_5H_{10}O$	87.080	69.070, 41.039
methylvinylketone	937	C_4H_6O	71.049	
methylethylketone	1017	C_4H_8O	73.065	
benzene	1006	C_6H_6	79.054	
m-xylene	983	C_8H_{10}	107.086	
1,3,5-trimethylbenzene	989	C_9H_{12}	121.101	
α-pinene	983	$C_{10}H_{16}$	137.132, 138.136	81.070
1,2,3-trifluorobenzene	1032	$C_6H_3F_3$	133.026	
1,2,4-trichlorobenzene	995	$C_6H_3Cl_3$	180.937, 182.934, 184.931	
hexamethylcyclo-trisiloxane (D3)	992	$C_6H_{18}Si_3O_3$	223.064, 224.063, 225.061	207.032, 208.032, 209.029
octamethylcyclo-tetrasiloxane (D4)	995	$C_8H_{24}Si_4O_4$	297.083, 298.082, 299.079	281.051, 282.051, 283.048
decamethylcyclo-pentasiloxane (D5)	995	$C_{10}H_{30}Si_5O_5$	371.101, 372.101, 372.105, 373.098	355.070, 356.070, 357.067

[1] *m/Q* values of isotopologues are only listed if their relative abundance is at least 10% of the most abundant isotopologue.

Table S3. Reaction rate constants used throughout this work.

Compound	**Formula**	**Reaction rate constant** [10^{-9} cm^3 s^{-1} $molecule^{-1}$]
methanol	CH_4O	2.20
acetonitrile	CH_3CN	3.10
acetaldehyde	C_2H_4O	3.03
acetone	C_3H_6O	3.25
isoprene	C_5H_8	1.85
methylvinylketone	C_4H_6O	2.72
methylethylketone	C_4H_8O	3.25
benzene	C_6H_6	1.97
2-methyl-buten-2-ol	$C_5H_{10}O$	1.85
m-xylene	C_8H_{10}	2.31
1,2,4-trimethylbenzene	C_9H_{12}	2.40
1,3,5-trimethylbenzene	C_9H_{12}	2.40
3-carene	$C_{10}H_{16}$	2.04
α-pinene	$C_{10}H_{16}$	2.04
1,2,4-trifluorobenzene	$C_6H_3F_3$	2.46
1,2,3-trifluorobenzene	$C_6H_3F_3$	2.46
1,2,4-trichlorobenzene	$C_6H_3Cl_3$	2.4
hexamethylcyclo- trisiloxane (D3)	$C_6H_{18}Si_3O_3$	2.16
octamethylcyclo-tetrasiloxane (D4)	$C_8H_{24}Si_4O_4$	2.99
decamethylcyclo-pentasiloxane (D5)	$C_{10}H_{30}Si_5O_5$	3.39

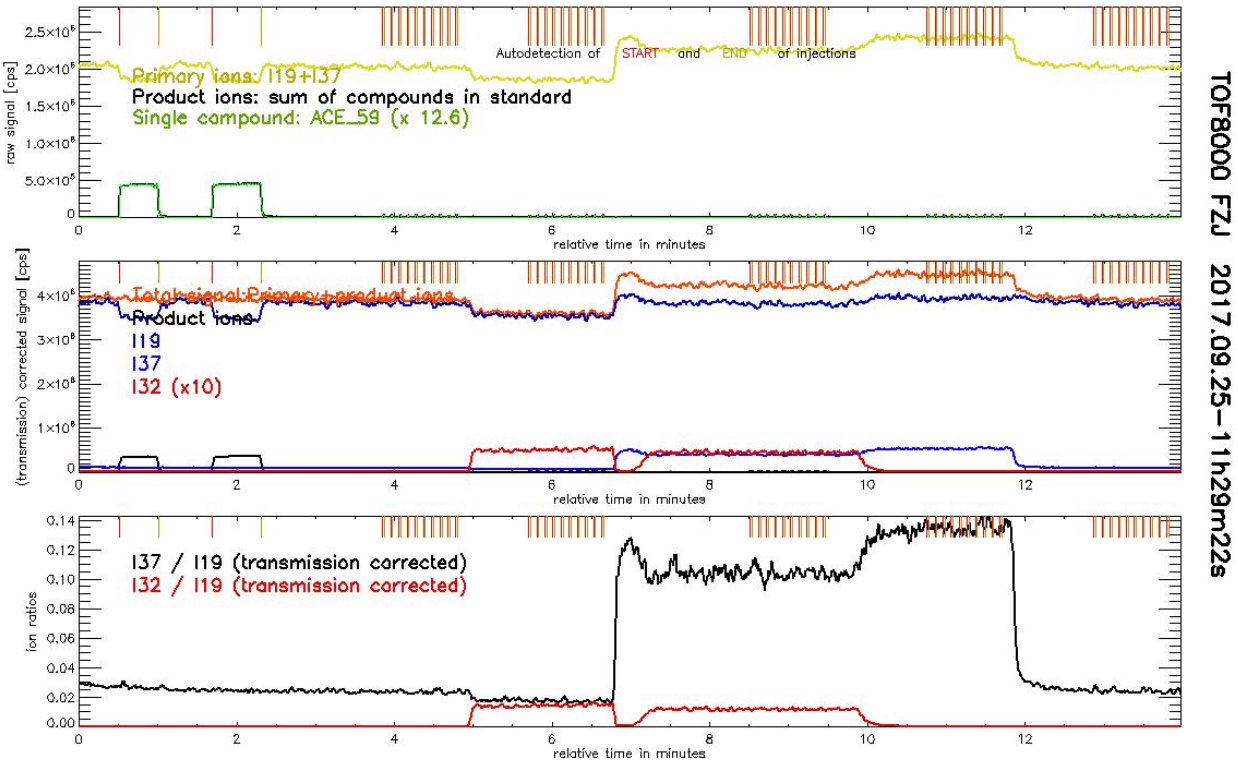

Figure S1. The PICAB standard addition protocol consisted of six operations: (i) two ~30 s periods of dynamic dilution of the gas standard into nitrogen (minutes 1.5 and 2), and five times 10 fast injections of gas standard from the sample loop into (ii) dry nitrogen (minute 4.5), (iii) dry air (minute 6), (iv) humidified air (minute 9), (v) humidified nitrogen (minute 11), and (vi) dry nitrogen (minute 13.5) as carrier gas. The start and end times of the standard additions are marked by red and yellow vertical lines at the top of each panel, respectively. The **top panel** shows raw ion count signal (counts per second, cps) of primary ions (yellow), the sum of all ions attributed to compounds in the gas standard (black), and of acetone (×12.6 in green) as example compound. The **center panel** shows corrected ion signals normalized to the mass dependent transmission of m/Q = 59 Th. Note that the sum of primary and product ions (orange trace) remains roughly constant during the sgas standard additions around minutes 0.75 and 2.0. The **bottom panel** shows ion ratios of $H_2OH_3O^+/H_3O^+$ (black) and O_2^+/H_3O^+ (red). The high O_2^+/H_3O^+ ratio (1.4 % and 1.2 %) is consistent with the ratio of 78.046 Th ($C_6H_6^+$ from the reaction of benzene with O_2^+) to 79.054 Th (protonated benzene produced by H_3O^+), whichh was 1.1 % and 1.0 % for the injections in dry and humidified air around minutes 6 and 9, respectively.

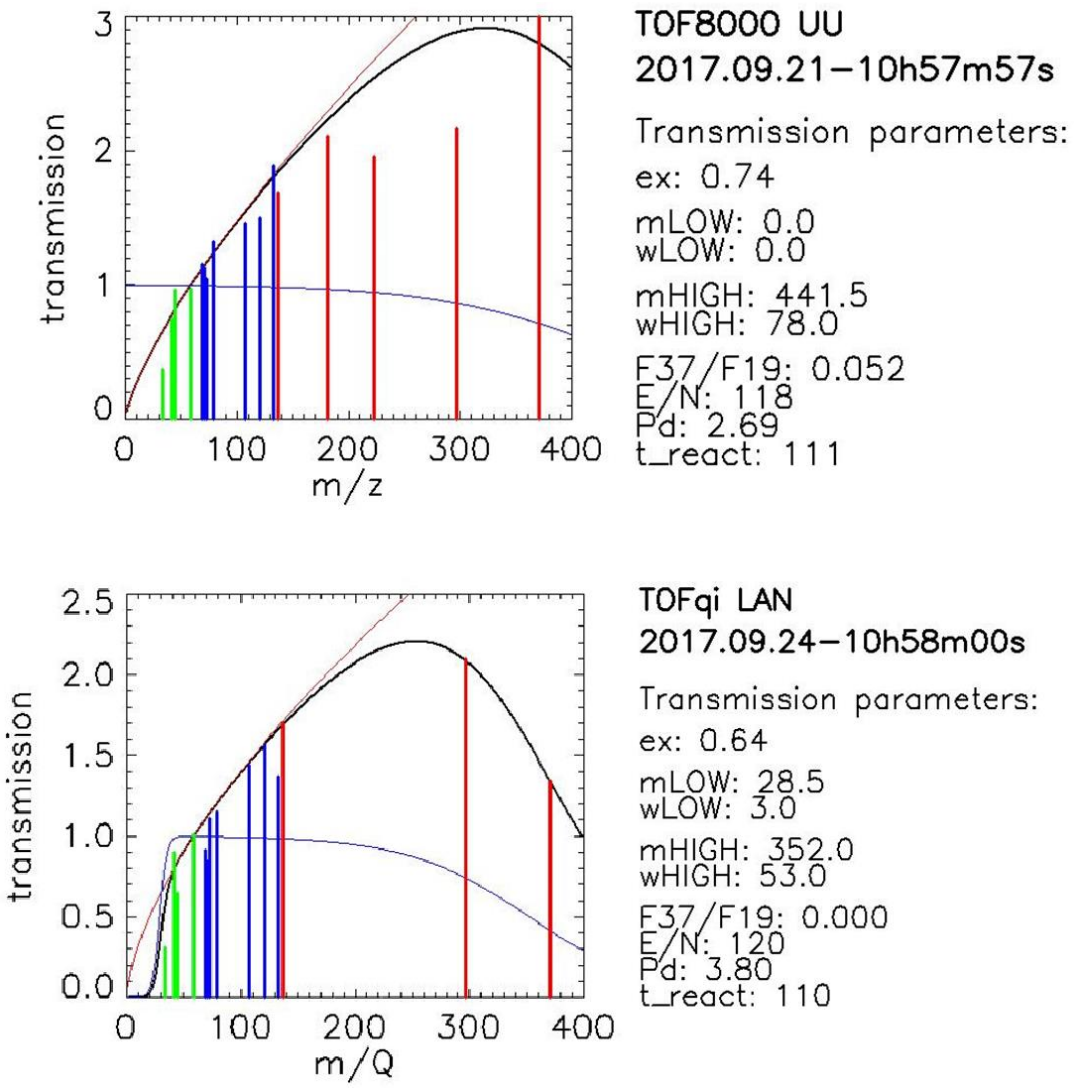

Figure S2: Two example retrievals of the transmission. The red line represents the characteristics in the medium *m/Q* range, and the blue line is the correction at low and high *m/Q*. The retrieved transmission is plotted in black. Green, blue, and red bars show the *m/Q* values of compounds that have been used to optimize for the low, medium, and high *m/Q* range, respectively. The height of the bars relates to the ratio measured/expected sensitivity multiplied with the transmission at the respective *m/Q* value, so that all bars should touch the transmission curve if the reaction kinetics model is 100 % correct. The lower chart shows a retrieval that could optimise the ratio measured/expected sensitivity, whereas this was not possible in the upper chart, where the algorithm optimised by evenly distributing the error between compounds at *m/Q* = 297 Th and *m/Q* = 371 Th (D4 and D5 siloxanes).

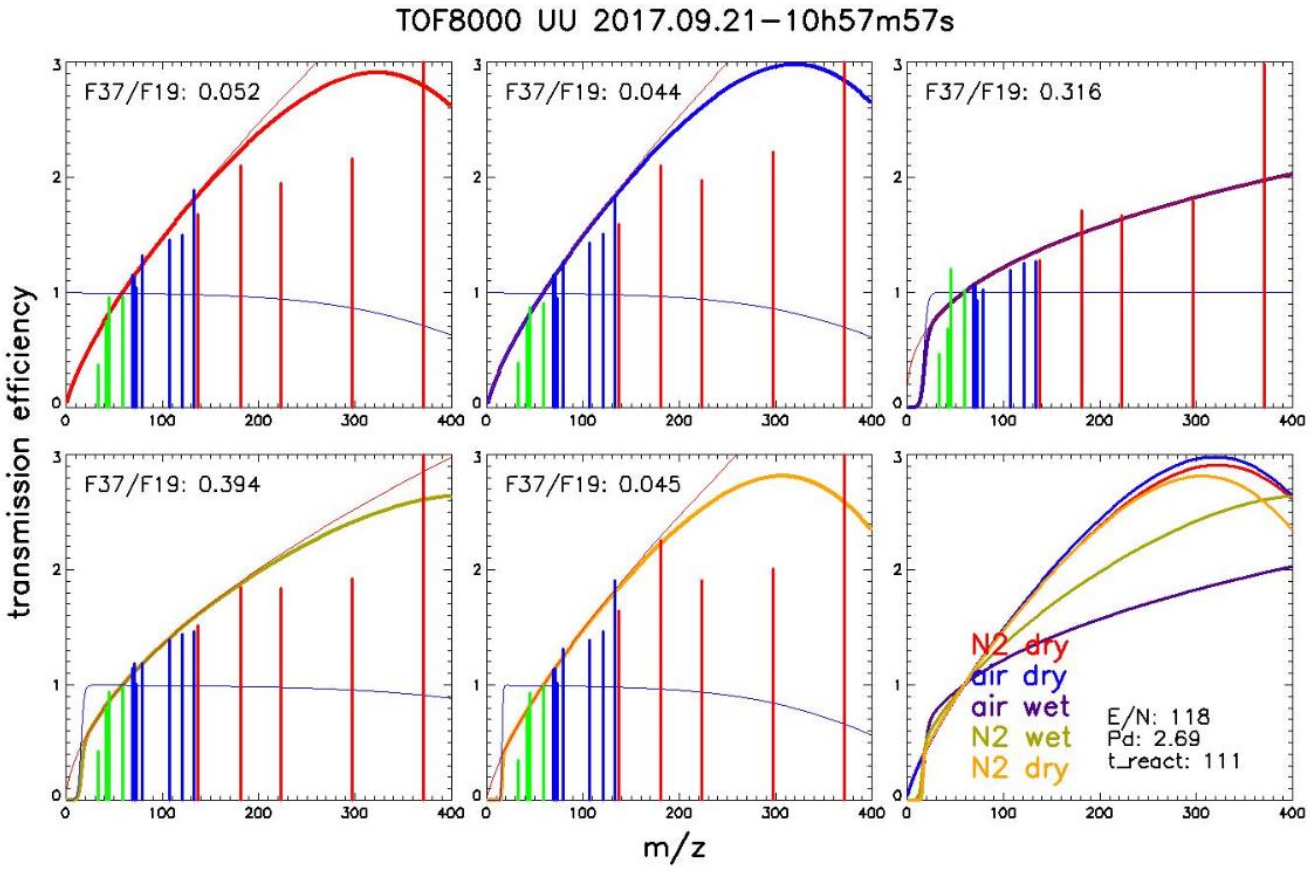

Figure S3. Five transmission retrievals for a full calibration protocol of 50 injections using dry N_2, dry air, humidified air, humidified N_2, and dry N_2 as carrier gas for 10 subsequent injections. For this study only the first 10 injections were used for the transmission retrieval. However, the sequence of the 5 retrievals shown here demonstrates the robustness of the algorithm for dry carrier gas and different results when humidified carrier gas is used. We interpret this to be an effect of unaccounted reaction kinetics with water hydronium clusters that are more abundant under humidified conditions.

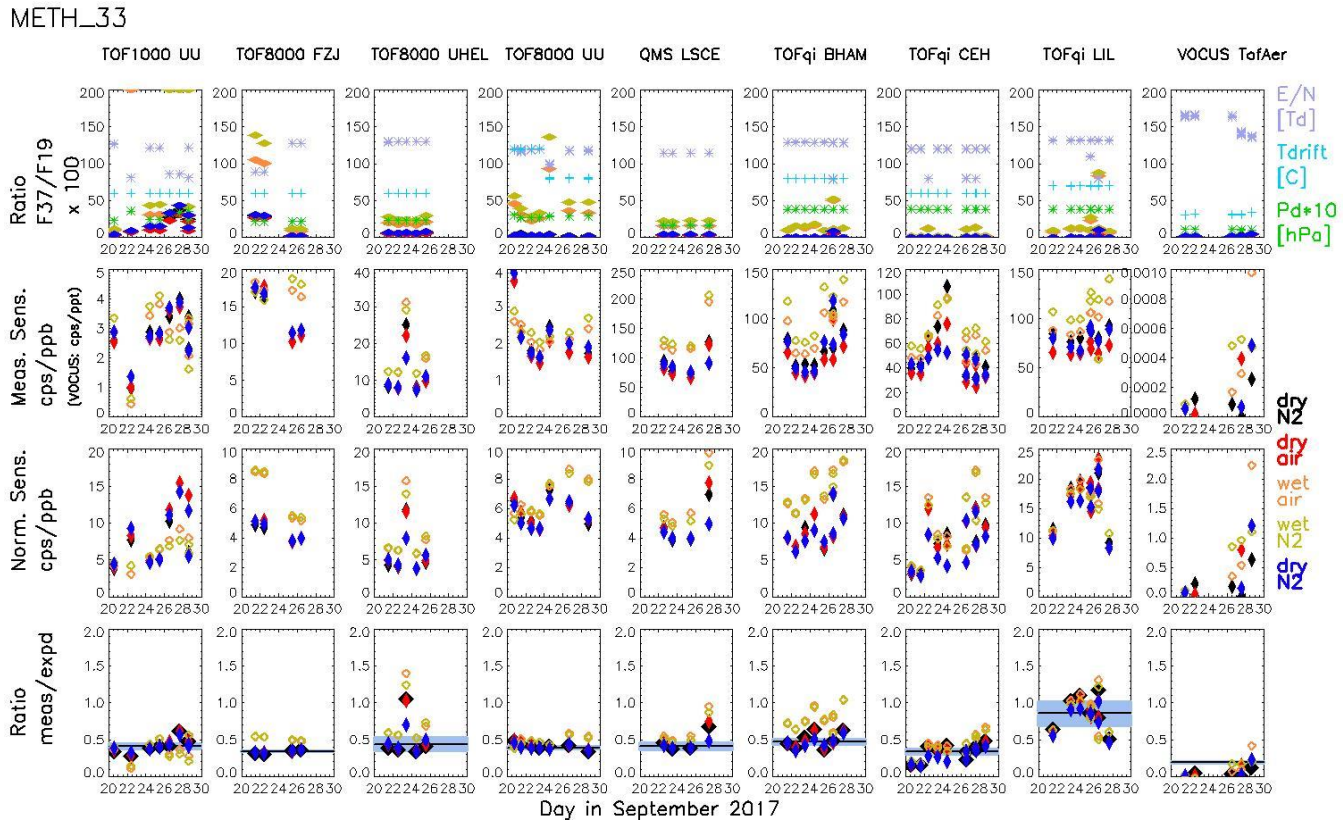

Figure S4. Summary for all measurements of methanol following our calibration protocol. Individual instruments are shown in the columns. The ***first-row*** panels show the ratio of primary ions $H_2OH_3O^+$ to H_3O^+ as well as operating conditions of the instruments (temperature, ℃, pressure in the drift tube, hPa, and *E/N* , Td, i.e. 10^{17} Vm^2). The ***second-row*** panels show the measured sensitivity of methanol for all instruments. The ***third-row*** panels show the normalized sensitivity, i.e. the measured sensitivity normalized to a transmission corrected primary ion signal (sum of H_3O^+ + $H_2OH_3O^+$) of 10^6 counts per second. The ***fourth-row*** panels show the ratio of the measured to expected sensitivity. The median ratio and the standard deviation of all ratios using dry carrier gas is plotted as black vertical line and grey shade, respectively. The colours and markers represent the different carrier gases. Humidified injections are depicted with open markers (orange and yellow-green for air and nitrogen, respectively); filled markers depict calibrations in dry carrier gas (black, red, and blue for nitrogen, air, and nitrogen, respectively).

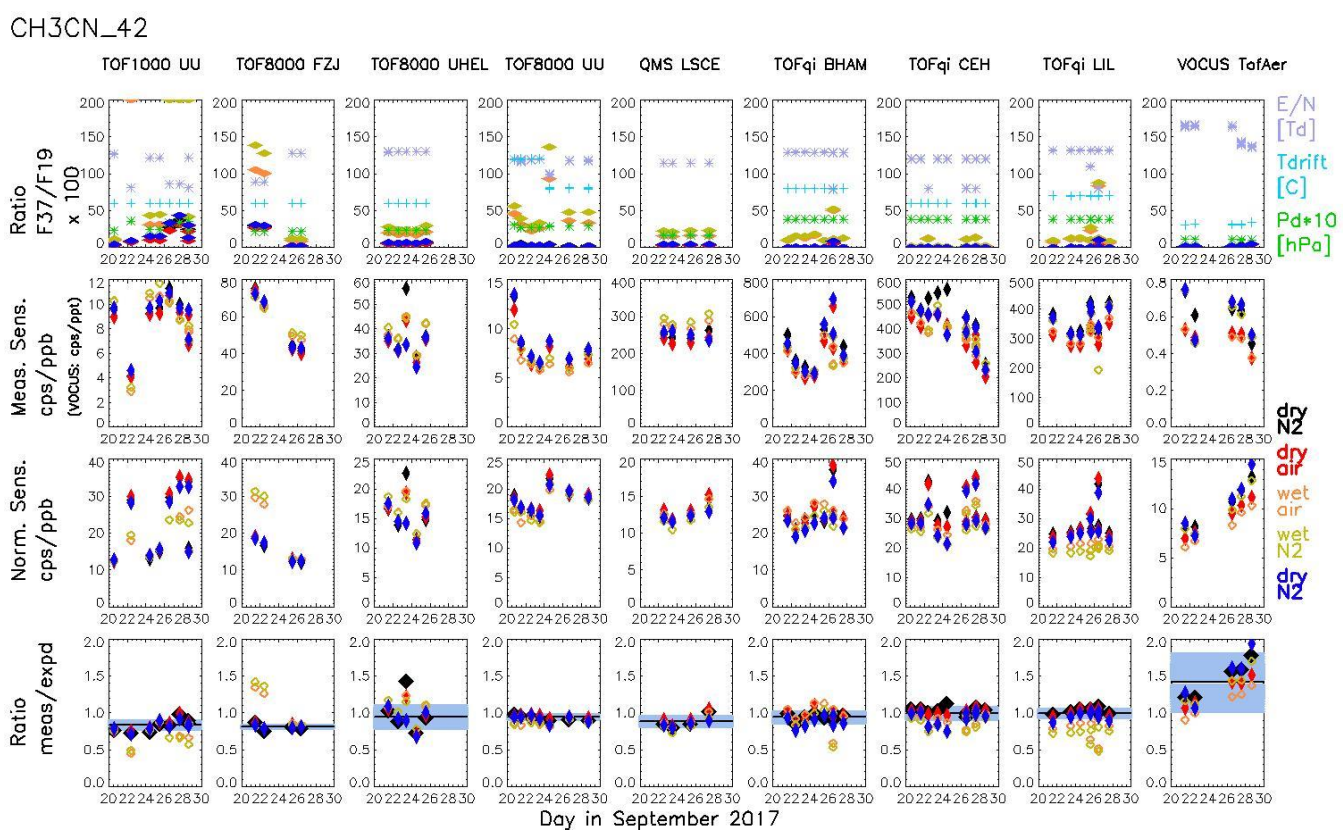

Figure S5. Same as in Figure S4 but for acetonitrile.

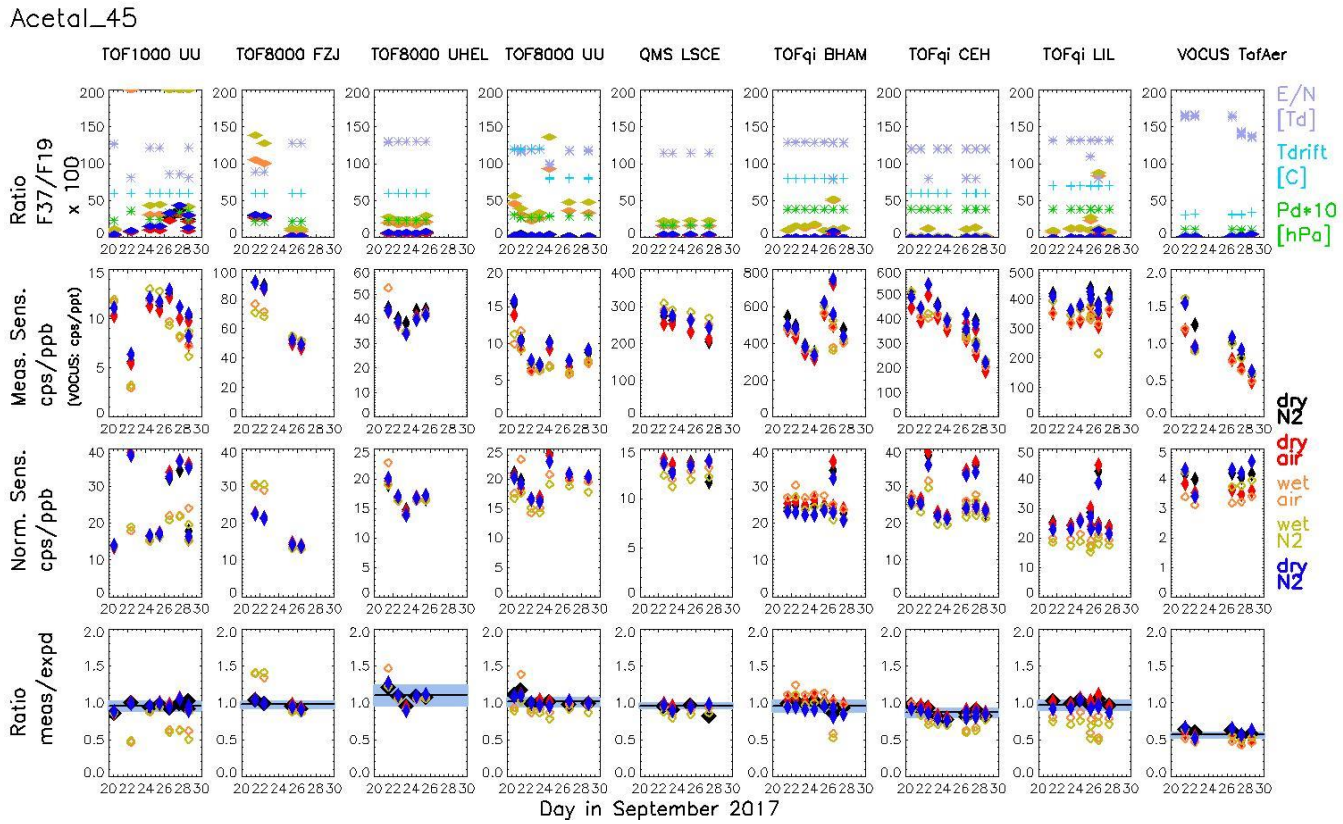

Figure S6. Same as in Figure S4 but for acetaldehyde.

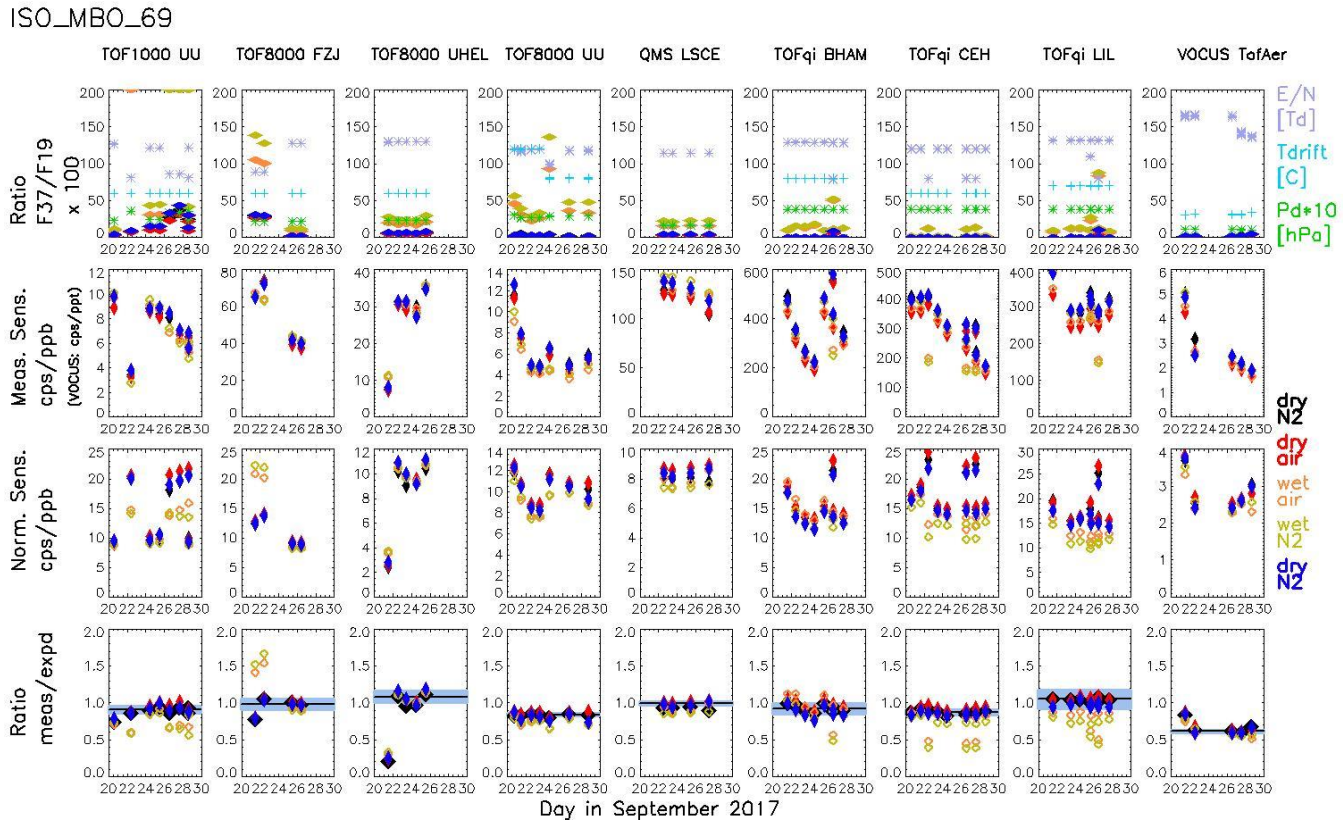

Figure S7. Same as in Figure S4 but for isoprene (September 22 onwards) or MBO (before September 22).

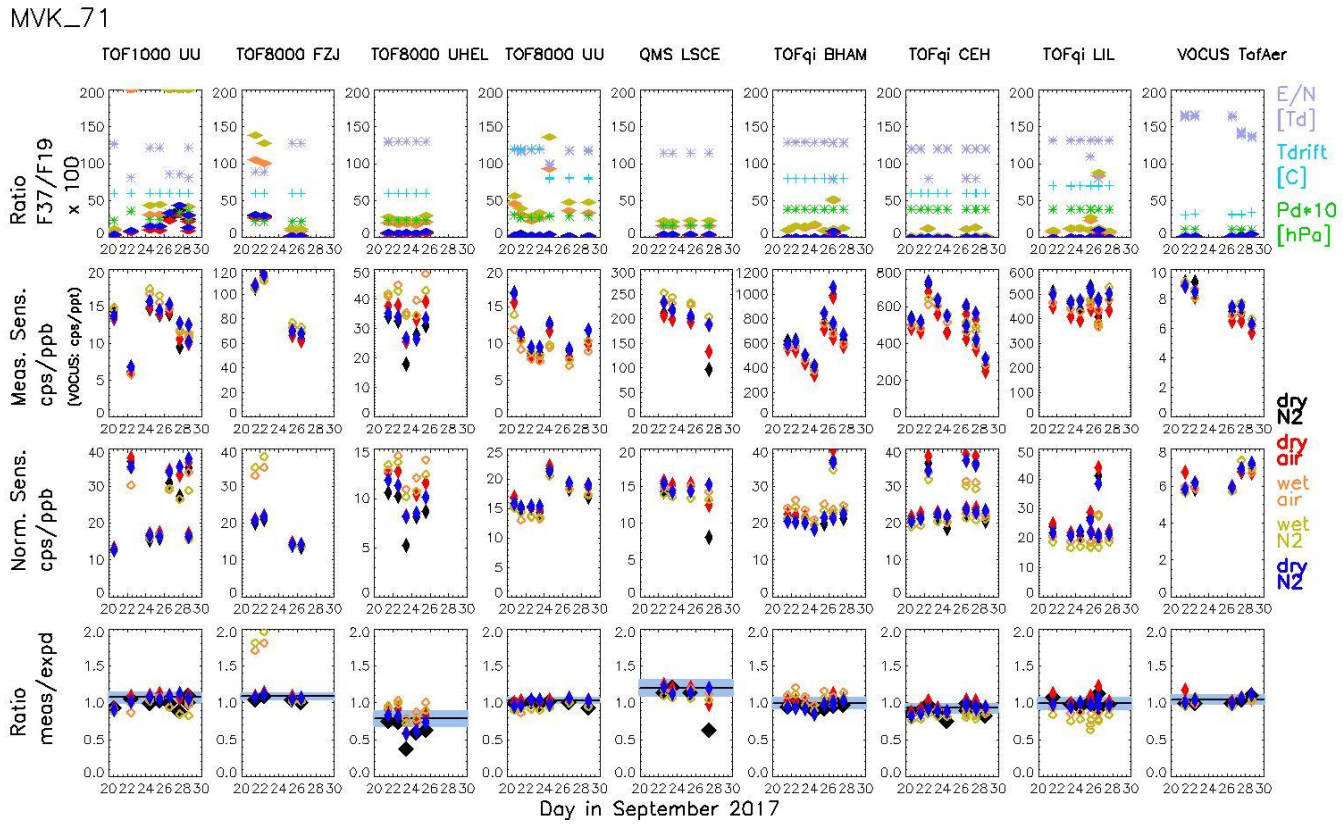

Figure S8. Same as in Figure S4 but for methylvinylketone.

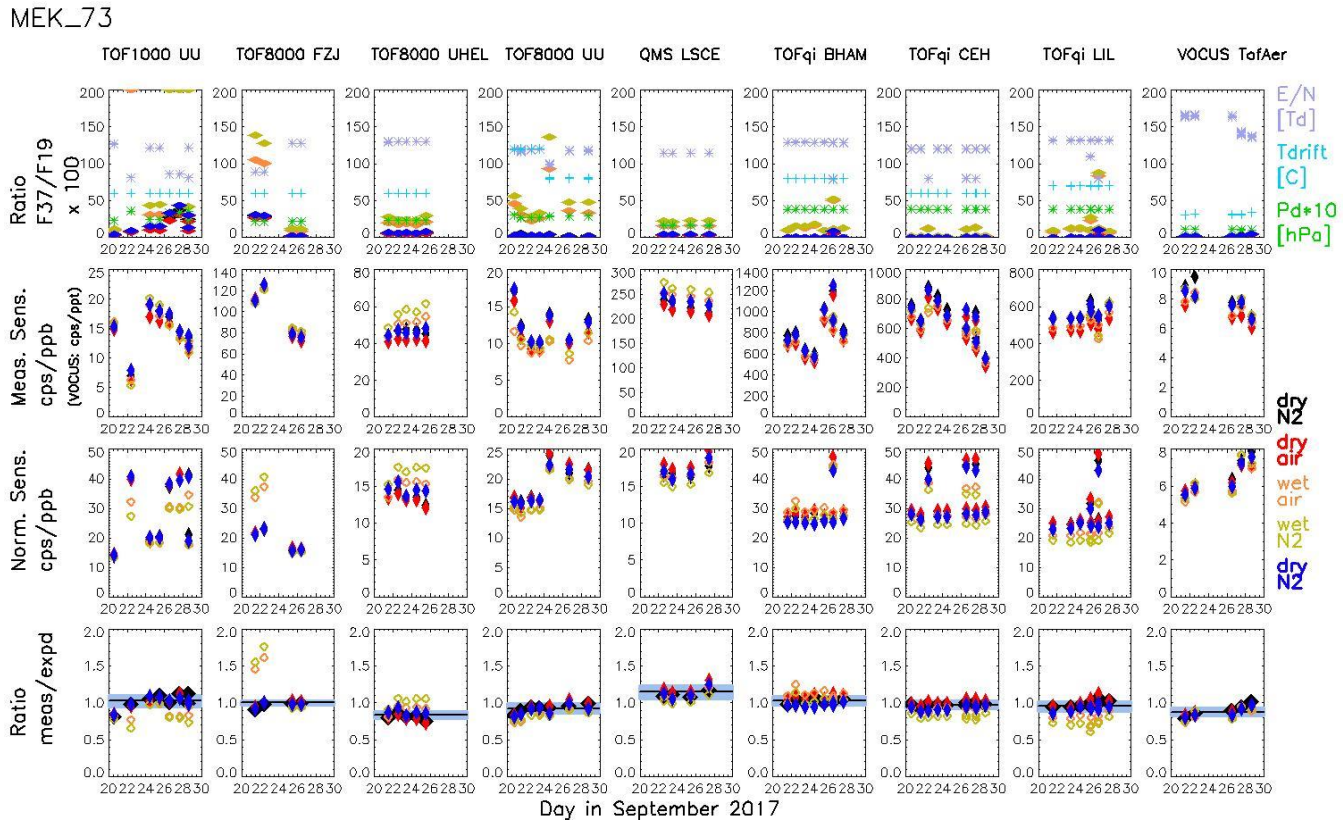

Figure S9. Same as in Figure S4 but for methylethylketone.

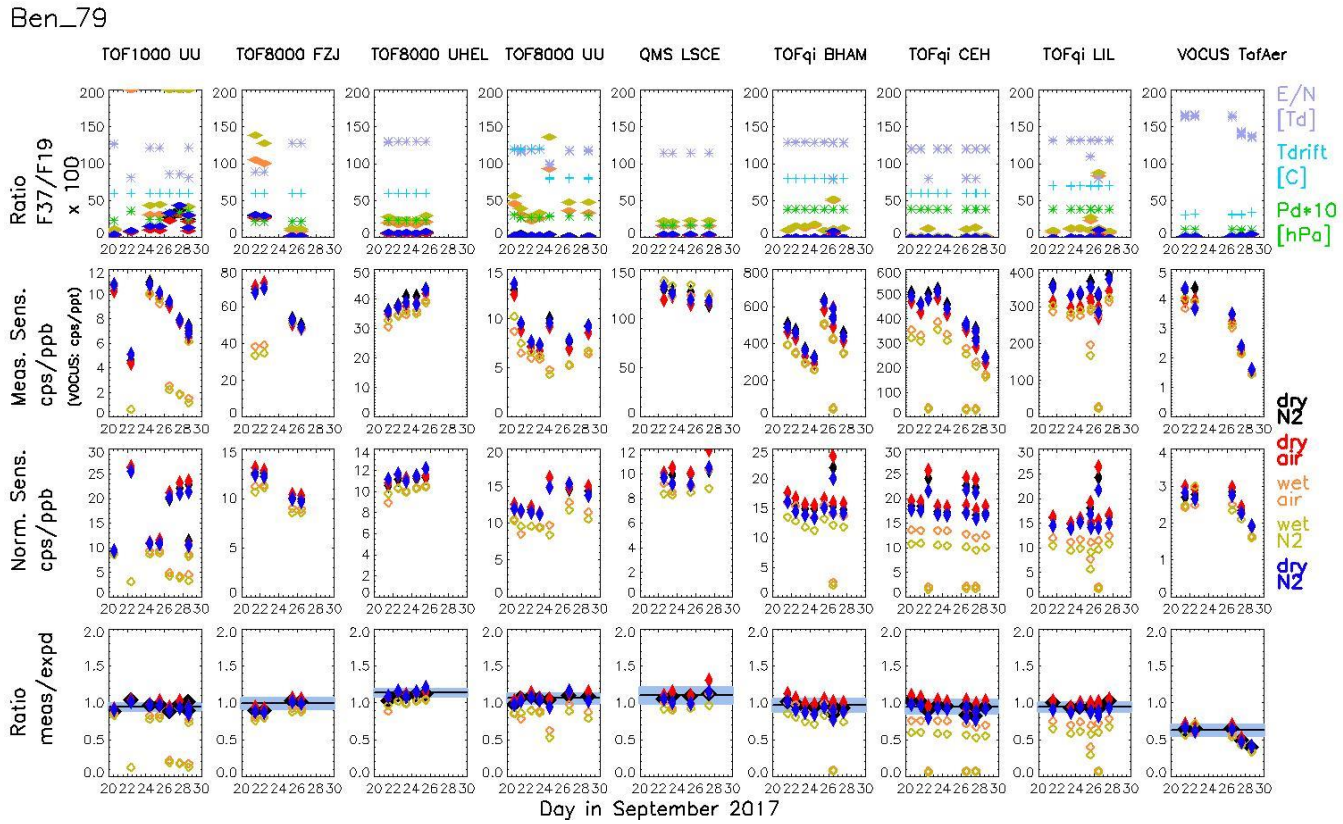

Figure S10. Same as in Figure S4 but for benzene.

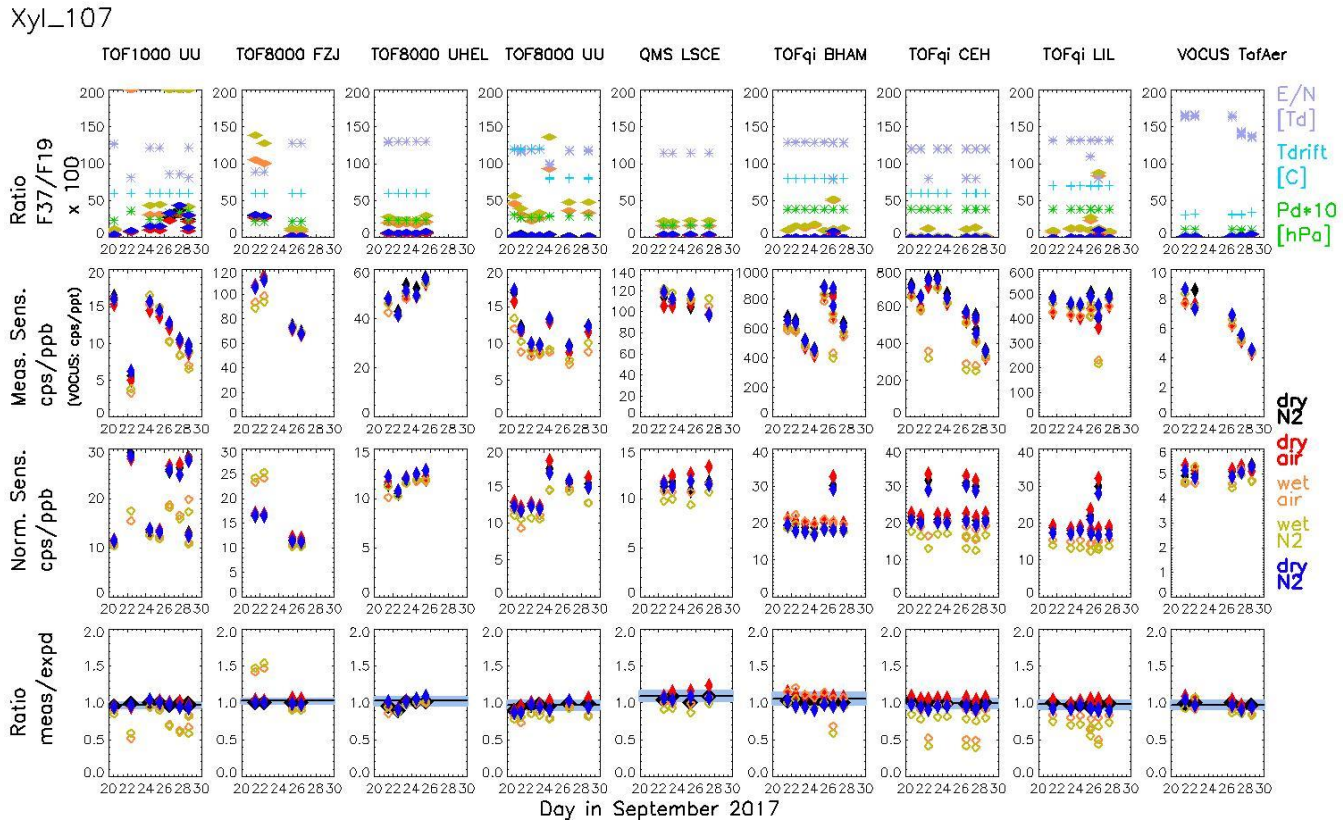

Figure S11. Same as in Figure S4 but for m-xylene.

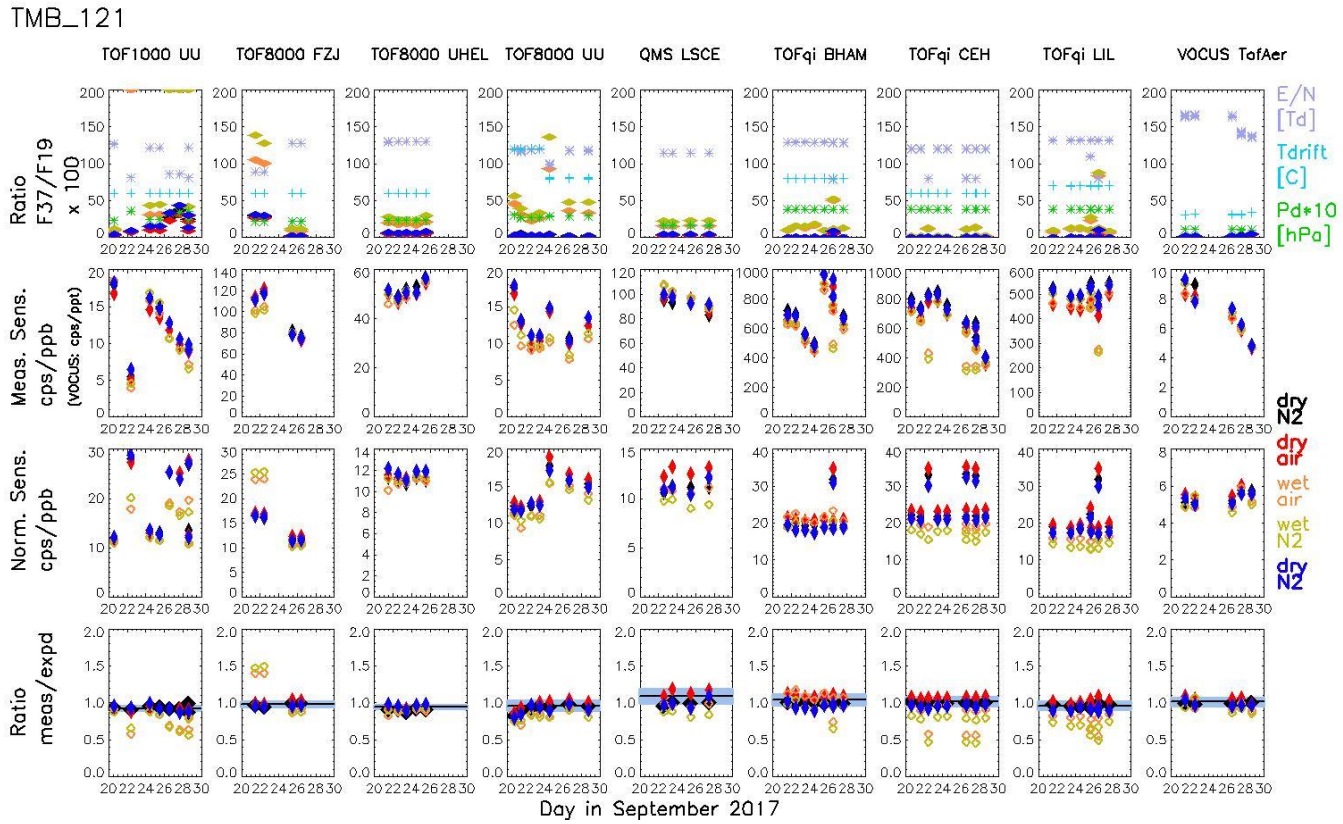

Figure S12. Same as in Figure S4 but for 1,2,4-trimethylbenzene (September 22 onwards) or 1,3,5-trimethylbenzene (before September 22).

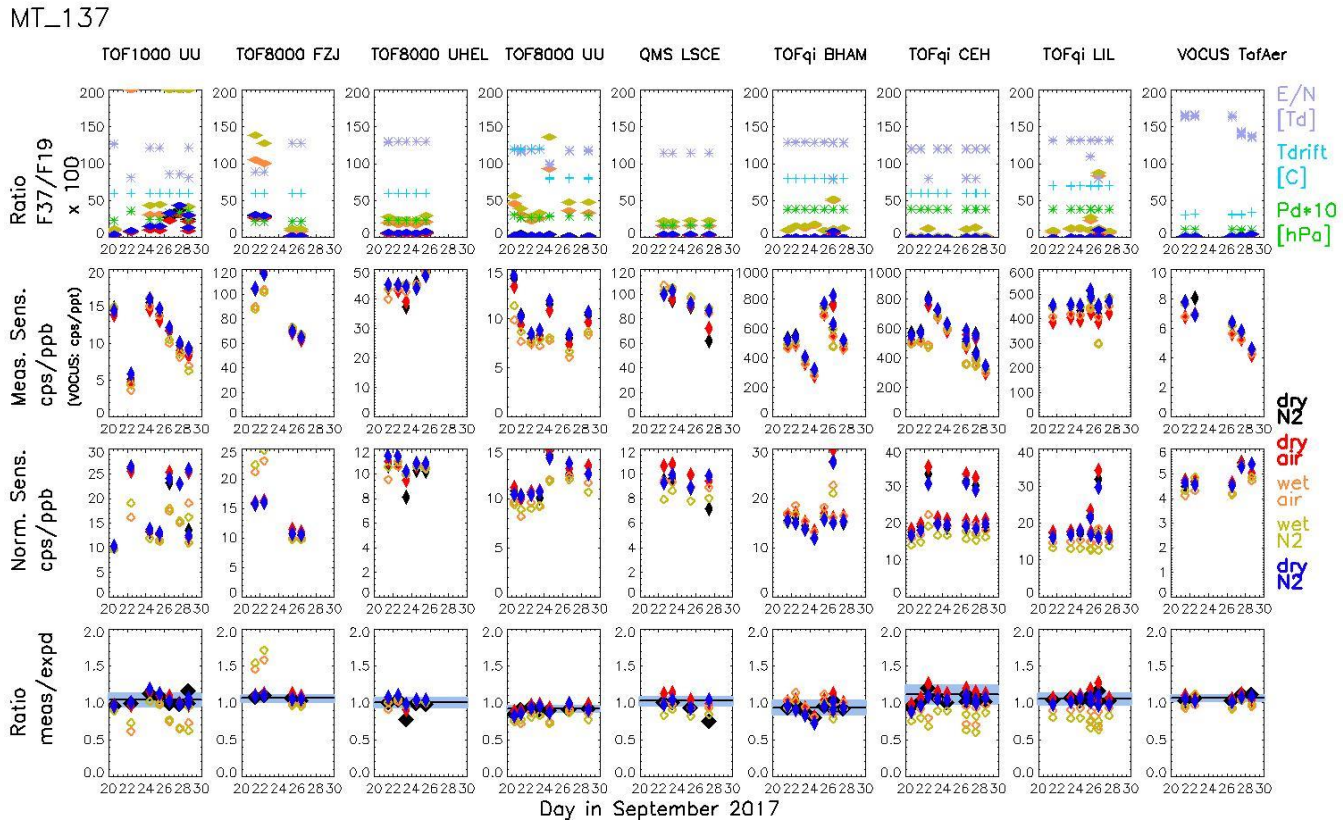

Figure S13. Same as in Figure S4 but for 3-carene (September 22 onwards) or α-pinene (before September 22).

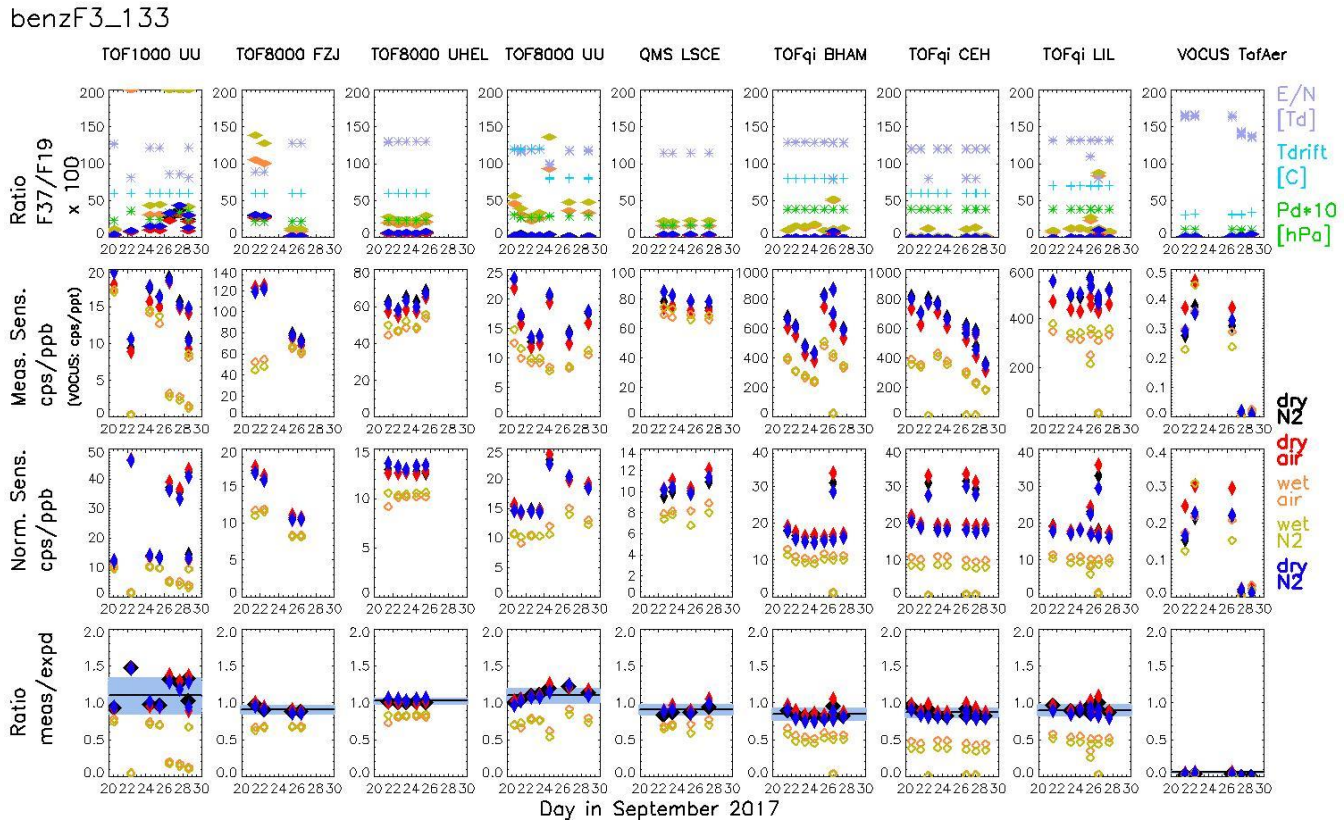

Figure S14. Same as in Figure S4 but for 1,2,4-trifluorobenzene (September 22 onwards) or 1,2,3-trifluorobenzene (before September 22).

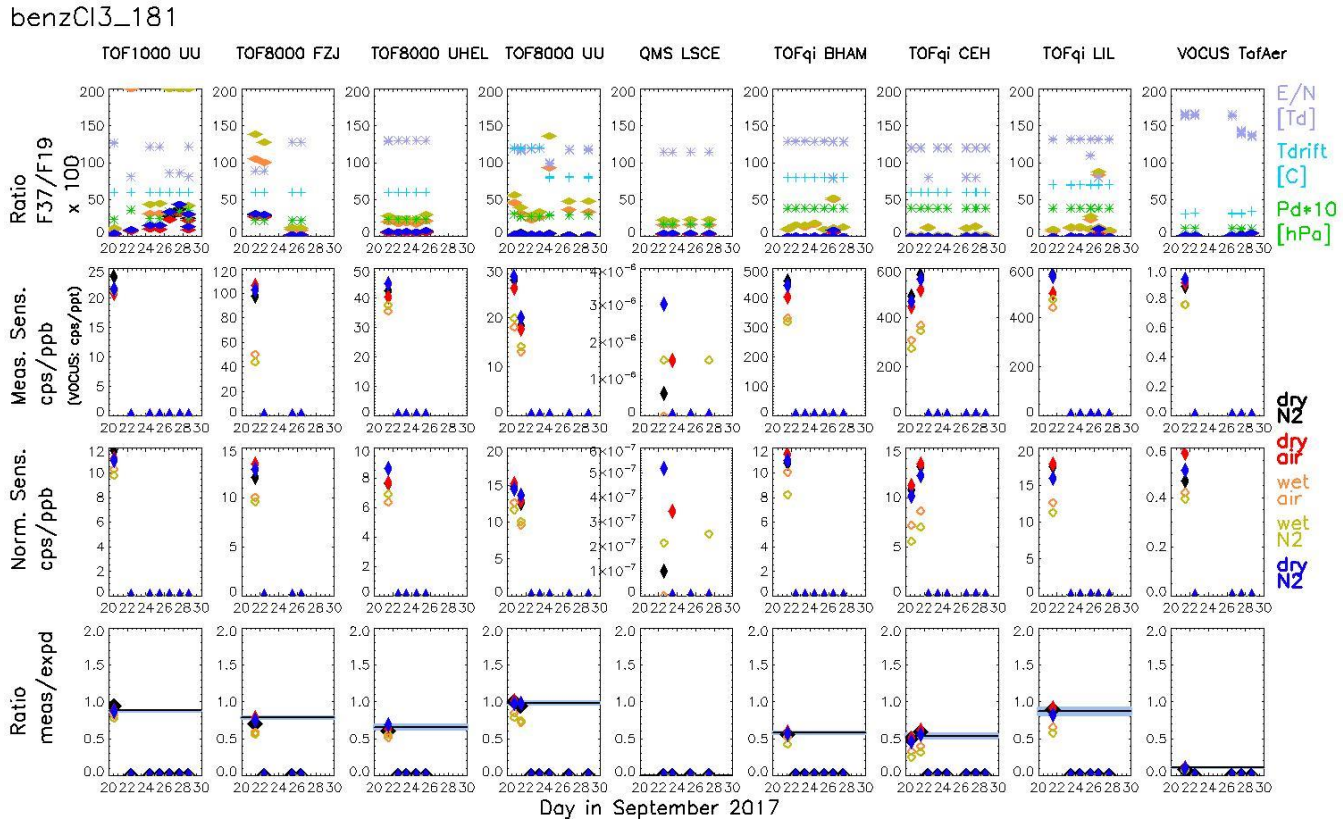

Figure S15. Same as in Figure S4 but for 1,2,4-trichlorobenzene (before September 22).

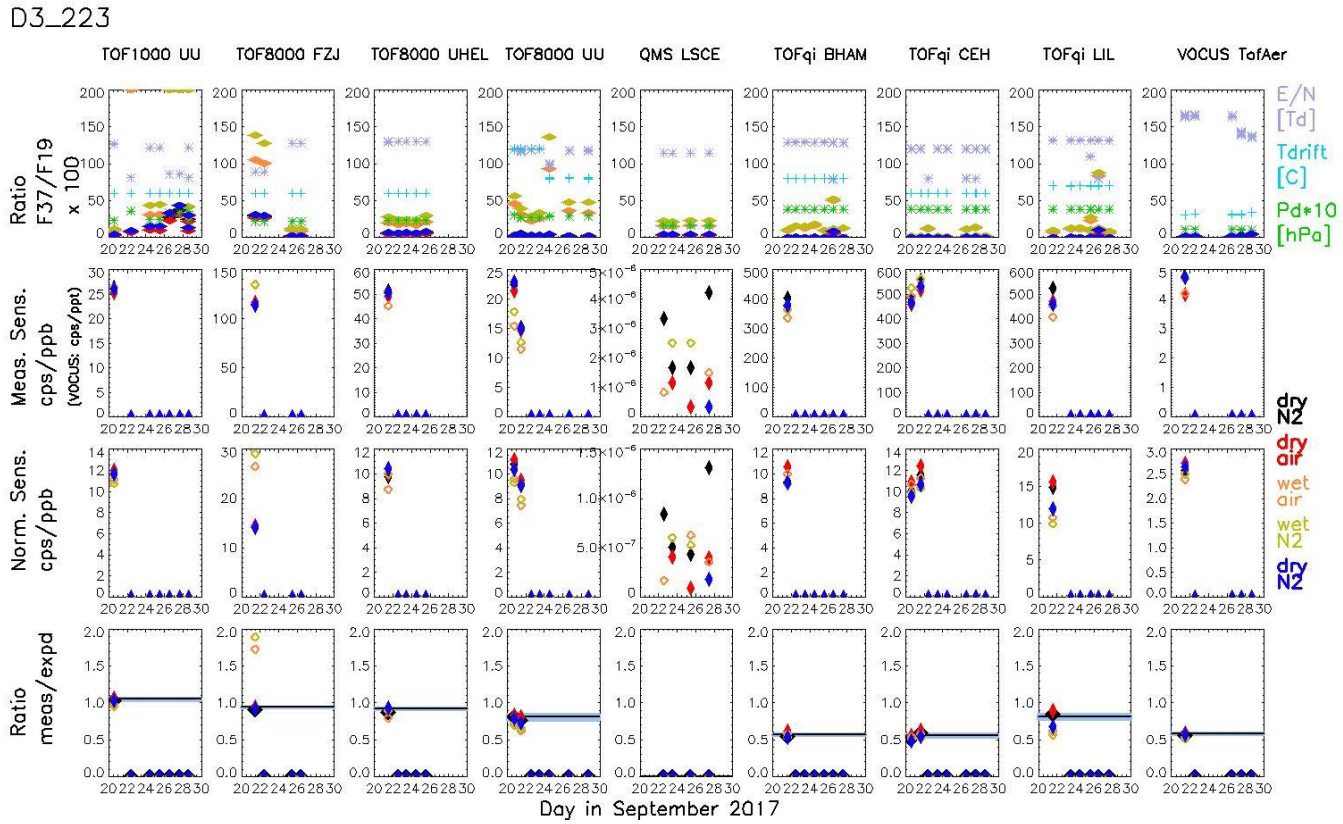

Figure S16. Same as in Figure S4 but for hexamethylcyclotrisiloxane (D3) (before September 22).

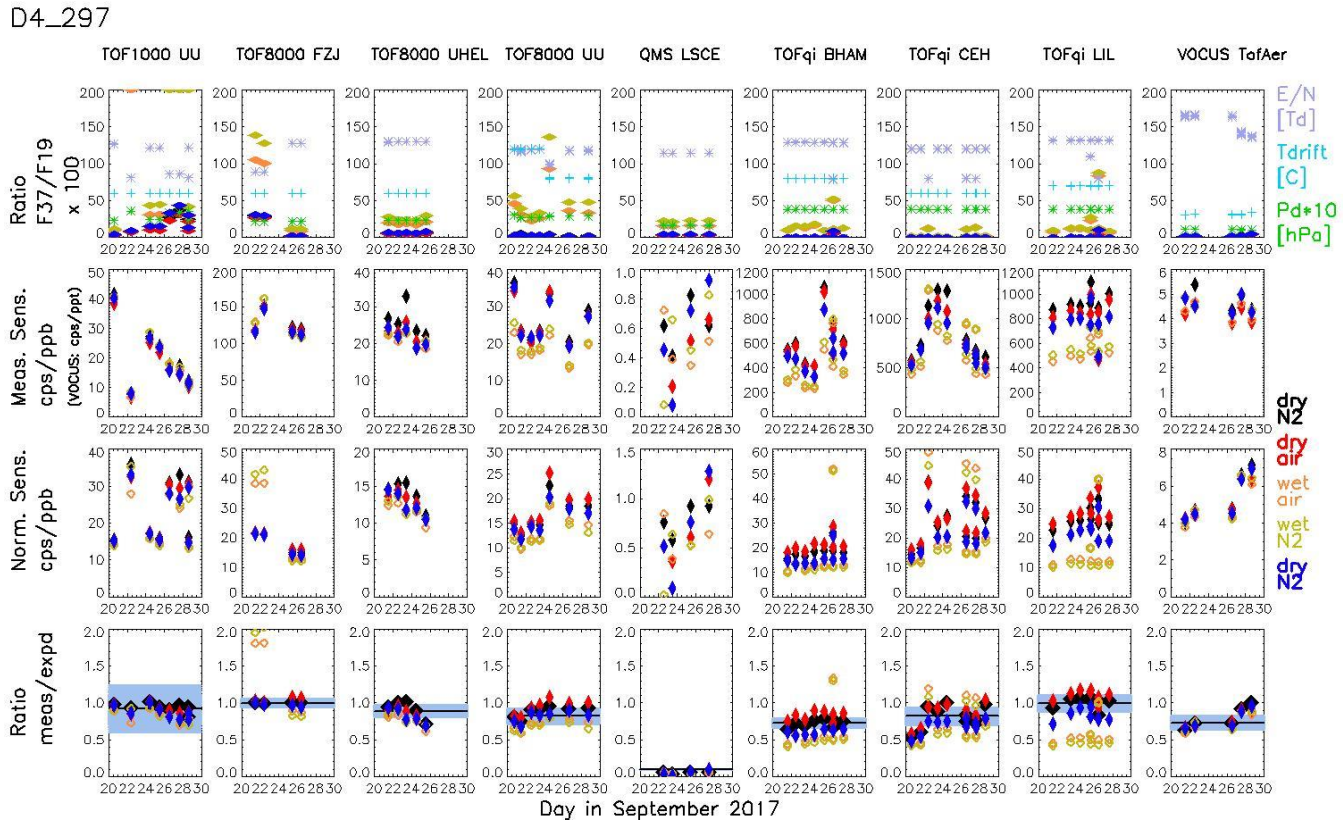

Figure S17. Same as in Figure S4 but for octamethylcyclotetrasiloxane (D4).

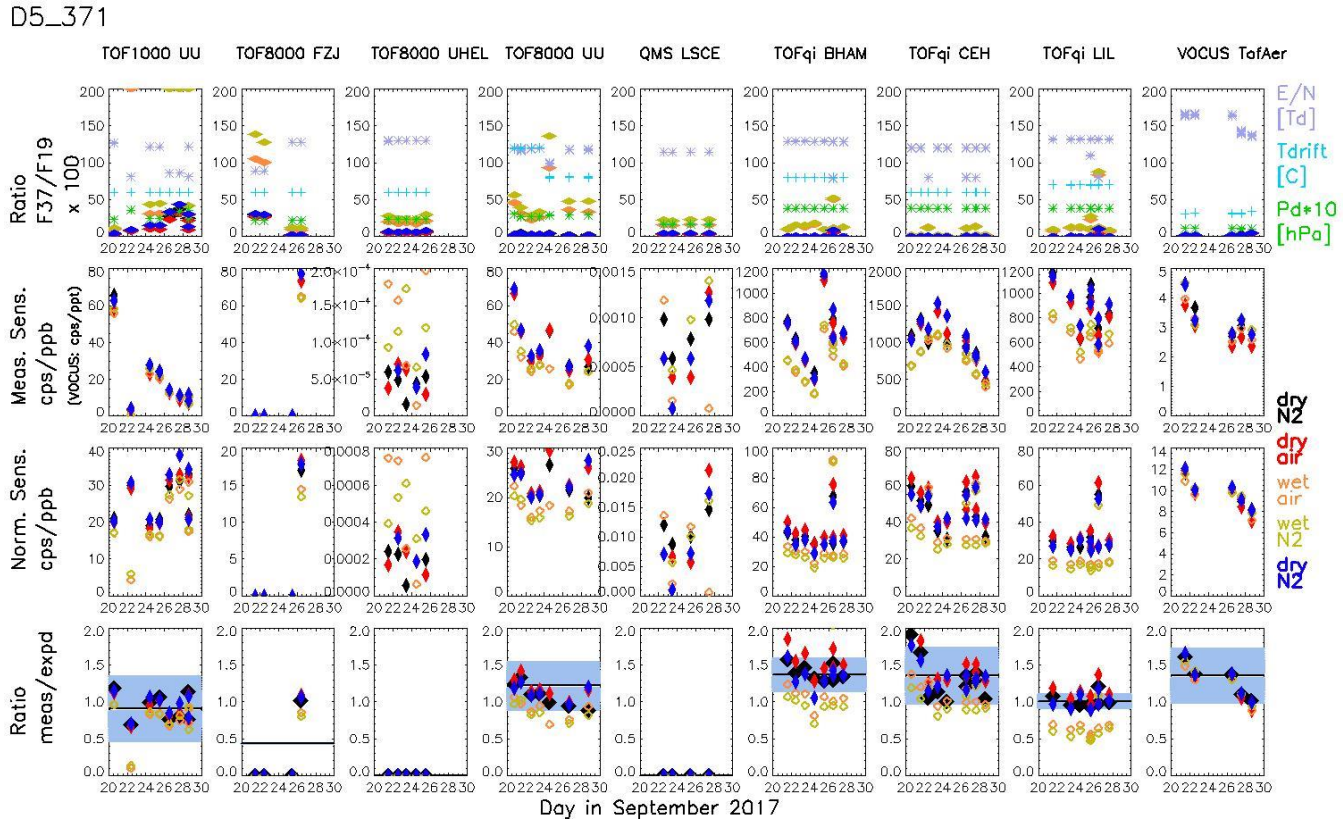

Figure S18. Same as in Figure S4 but for decamethylcyclopentasiloxane (D5). The TOF settings for the instruments 'FZJ'and 'UHEL' covered only ions up to ~320 Th (except the last measurement for 'FZJ'). D5 could not be detected in the 'LSCE' instrument due to the limitations of the QMS analyser.